

# Kinetics of titanium extraction at hydrometallurgical fluoridation of titanomagnetite ore

**V. I. Sachkov**, Doctor of Chemical Sciences, Associate Professor, Head of Laboratory<sup>1</sup>, e-mail: vicsachkov@gmail.com

**R. O. Medvedev**, Candidate of Technical Sciences, Senior Researcher<sup>1</sup>, e-mail: rodionmedvedev7@gmail.com

**R. A. Nefedov**, Candidate of Chemical Sciences, Senior Researcher<sup>1</sup>, e-mail: ronef88@yandex.ru

**V. V. Orlov**, Junior Researcher<sup>2</sup>, e-mail: vvorlov92@mail.ru

<sup>1</sup> National Research Tomsk State University, Tomsk, Russia.

<sup>2</sup> Institute for Problems of Chemical and Energy Technologies of the Siberian Branch of the Russian Academy of Sciences, Biysk, Russia.

This paper presents a study of the kinetics of titanium leaching during fluorammonium hydrometallurgical processing of titanomagnetite ores from the China deposit. A series of experiments was conducted to determine the kinetic parameters over a range of process durations. Two leaching solutions were employed to investigate the kinetics of the process, and the composition and concentration of these solutions were identified as optimal for achieving the maximum level of titanium and vanadium extraction into solution. The concentration of  $(\text{NH}_4)^+$  in both solutions was 0.4 mol/L, while the concentration of  $(\text{F})^-$  for solution 1 was 0.8 mol/L and for solution 2 was 0.9 mol/L. It was observed that the rate of titanium recovery declines with the passage of time. At approximately 10 hours, the rate of recovery reaches a plateau. In the initial five hours of leaching, the graph is linearised in the coordinates of the 'shrinking sphere' model. The results of calculations for the second section, with a duration of between 5 and 25 hours, are linearised in the coordinates of the Yander equation. The value of the apparent activation energy falls within the range  $E_a \in (30; 71)$  kJ/mol, indicating that the leaching process occurs in a kinetic regime.

**Key words:** titanomagnetite ores, hydrometallurgical process, leaching, titanium-vanadium concentrates, iron concentrates, leaching kinetics.

**DOI:** 10.17580/nfm.2024.02.02

## Introduction

Titanomagnetite is a mineral widely distributed in the subsurface, belongs to the class of complex oxides and is usually the main ore mineral of most magmatic iron deposits, spatially and genetically associated with ultramafic and mafic rocks [1]. Titanomagnetite ores are considered one of the most promising types of unconventional ores and are an important source of iron and titanium, the content of which can vary widely [2, 3]. Titanomagnetite is typically a polymineral formation, comprising a mixture of different minerals. Magnetite ( $\text{Fe}_3\text{O}_4$ ) acts as a matrix, and ilmenite ( $\text{FeTiO}_3$ ), ulvospinel ( $\text{Fe}_2\text{TiO}_4$ ) and magnesian ulvospinel ( $\text{Mg}_2\text{TiO}_4$ ) act as inclusions in the matrix [4]. The amount of iron varies from 50 to 68% due to the presence of inclusions of other minerals and isomorphic impurities in titanomagnetite [5, 6]. Classification of titanomagnetite ore by the value of  $\text{TiO}_2$  content consists of three varieties: low-titanium (1–4%), medium-titanium (5–9%) and high-titanium (10–20%) [7, 8].

In consideration of the various methods of processing titanomagnetite ores, it was observed that although pyrometallurgical methods are widely employed in the processing of titanomagnetite, hydrometallurgical methods are gaining prominence. Concurrently, the established hydrometallurgical techniques are associated with several

drawbacks. Consequently, there is a keen pursuit of alternative approaches to titanomagnetite processing.

The utilisation of fluorine-containing reagents in the leaching of titanomagnetite facilitates the effective destruction of the crystal lattice of minerals, thereby enhancing the extraction of components into solution [12]. The fluorinating agents ammonium fluoride and ammonium hydrodifluoride possess several advantages, including the capacity for relatively straightforward recycling. Nevertheless, fluorination is frequently conducted at elevated temperatures and concentrations of the primary reagents, with subsequent product separation occurring via pyrohydrolysis. Despite the ability of such technologies to yield products with a high degree of purification, they necessitate the investment in costly hardware design and the introduction of a complex process [13, 14].

In the event of processing titanomagnetite ore via the heap leaching method, with the objective of obtaining an iron concentrate as the primary product and associated extraction of Ti, V, and other metals, a high degree of product purity is not a prerequisite. Consequently, fluoride stripping of raw materials can be conducted under milder conditions, thus circumventing the aforementioned drawbacks associated with this technology. Previously, we have conducted research on the processing of titanomagnetite ore based on the selective extraction of titanium and other

metals by a solution containing ammonium and fluorine ions, with variations in process parameters. This paper presents information on the leaching kinetics and titanium recovery rate. Ammonium fluoride or ammonium hydrofluoride leaching solutions with varying fluoride ion concentrations were selected for the study of process kinetics, based on the findings of previous research [15].

### Materials and methods

The research was conducted using samples of titanomagnetite ore from the Magnitny section of the China deposit. The ore was a lump material with a grain size of  $-100+30$  mm, which was subjected to crushing on a jaw crusher. Subsequently, the ore was pulverised, resulting in the acquisition of a sample comprising particles of a diameter less than 3 mm.

A qualitative X-ray phase analysis of the studied sample was conducted on an XRD-6000 X-ray diffractometer. The imaging parameters were as follows:  $\lambda$  (Cu  $K_{\alpha}$ ) = 0.154 nm, time constant  $\tau = 0.5$  s;  $2\theta = 15-85^{\circ}$ ; speed  $0.5^{\circ}/\text{min}$ . The phases were identified using the PDF 4+ databases, as well as the POWDER CELL 23 full-profile analysis program. **Table 1** illustrates the composition of the initial samples of titanomagnetite ore from the China deposit, delineating the proportions of the various phases present.

The content of elements in ore and their concentrations in solutions were determined by inductively coupled plasma mass spectrometry on ELAN spectrometer model DRC-e No. W1520501 according to the methodology of MBI No. 002-HMS-2009, FR.1.31.2010.06997. **Table 2** illustrates the concentration of the principal components in the initial samples of titanomagnetite ore.

The following reagents were employed in the hydro-metallurgical tests: hydrofluoric acid (analytical reagent grade, GOST 10484–78), ammonium fluoride (analytical reagent grade, GOST 4518–75), ammonium hydrofluoride (analytical reagent grade, GOST 9546–75), aqueous ammonia (analytical reagent grade, GOST 3760–79), and distilled water.

To examine the kinetics of the process, leaching solutions with varying fluoride ion concentrations were selected, as these demonstrated the most optimal levels of titanium and vanadium extraction. Leaching was conducted in 1000 mL polyethylene agitators under constant mechanical stirring at  $20 \pm 2^{\circ}\text{C}$ . The concentration of  $\text{NH}_4^+$  in both solutions was 0.4 mol/L, while the concentration of  $(\text{F})^-$  for Solution 1 was 0.8 mol/L and for Solution 2 it was 0.9 mol/L. The mass ratio of the solid and liquid phases during agitation leaching was 1 : 3. The duration of the process varied between one and twenty-five hours. The extraction of titanium was evaluated through the analysis of the chemical composition of the leaching solution using the ICP-MS method.

### Results and discussion

The developed technology is based on the selective extraction of titanium from raw materials by a solution containing ammonium and fluorine ions, with the process

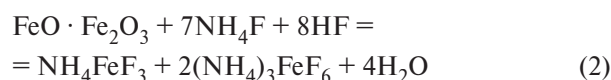
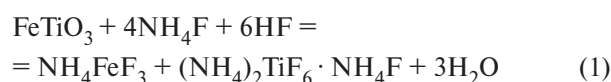
Table 1  
Ore phase composition (%)

Detected phases	Content, wt. %
Magnetite ( $\text{Fe}_3\text{O}_4$ )	40
Ilmenite ( $\text{FeTiO}_3$ )	25
Cronstedtite ( $\text{Fe}_3(\text{FeSi})\text{O}_4(\text{OH})_5$ )	15
Magnesioferrite ( $\text{MgFe}_2\text{O}_4$ )	8
Other	12

Table 2  
Content of main components in feed ore

Element	Content, wt. %
Iron (Fe)	53.00
Titanium (Ti)	8.82
Aluminum (Al)	2.08
Magnesium (Mg)	1.81
Calcium (Ca)	0.74
Vanadium (V)	0.48

parameters undergoing variation. The extraction of titanium from ore into solution results in the formation of two distinct products: a solid fraction, comprising iron concentrate, which represents a significant material in the metallurgical industry, and a liquid fraction, comprising titanium (titanium-vanadium) concentrate, which serves as a source of both titanium and vanadium. Consequently, the higher the iron content and the lower the titanium content of the iron concentrate, the higher the quality will be. In contrast, this is not the case with titanium concentrate. Consequently, the primary challenge was to separate these two components in a highly selective manner. The most probable schemes for the leaching process of the main minerals are as follows:



The processing modes were selected on the basis of key process parameters, including the iron and titanium content of the concentrate, their ratio, and the titanium recovery rate. The most efficacious results of the hydro-metallurgical processing of titanomagnetite ore are presented in **Table 3**.

The results of the experiment, which varied the leaching time, are presented in **Fig. 1**.

As illustrated in **Fig. 1**, the kinetic curves exhibit a parabolic profile. The analysis of the experimental data indicated that as the duration of the leaching process increased, the degree of titanium extraction also increased. The exponential phase of titanium extraction is observed during the first five hours of interaction. After 10 hours, the curves reach a plateau, and the degree of titanium

Table 3  
Effective indicators of titanomagnetite ore processing process

Leaching solution composition	Mass fraction in iron concentrate (solid phase), %		Degree of Ti extraction into solution, %	Fe/Ti ratio in iron concentrate (solid phase)
	Fe	Ti		
1 <sup>st</sup> Solution ( $C_M(\text{NH}_4)^+ = 0.4 \text{ mol/L}$ , $C_M(\text{F})^- = 0.8 \text{ mol/L}$ )	66.47	4.03	53	16.5
2 <sup>nd</sup> Solution ( $C_M(\text{NH}_4)^+ = 0.4 \text{ mol/L}$ , $C_M(\text{F})^- = 0.9 \text{ mol/L}$ )	67.34	3.1	64	21.7

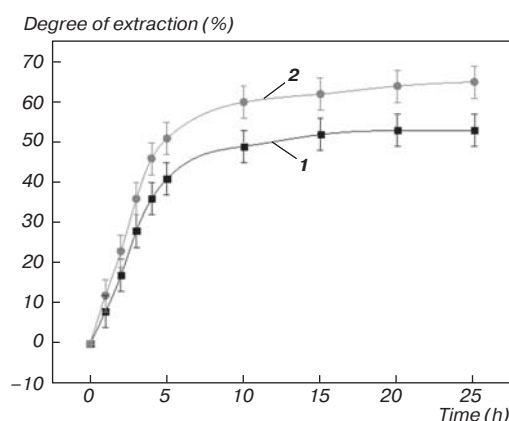


Fig. 1. Graph of dependence of the degree of titanium extraction into solution on the duration of the process:  
1 –  $C_M(\text{NH}_4)^+ = 0.4 \text{ mol/L}$ ,  $C_M(\text{F})^- = 0.8 \text{ mol/L}$ ; 2 –  $C_M(\text{NH}_4)^+ = 0.4 \text{ mol/L}$ ,  $C_M(\text{F})^- = 0.9 \text{ mol/L}$

extraction remains relatively constant, ranging from 49% to 53% and from 60% to 65% for the first and second solution, respectively. In light of these observations, it was decided to divide the kinetic dependences into two time intervals of the process: the first interval  $\tau = 5 \text{ h}$ , during which the transition of titanium into solution is active,

and the second interval  $\tau = 5\text{--}25 \text{ h}$ , during which the degree of titanium extraction changes slowly.

The experimental data was linearised in accordance with the equations of formal kinetics of topochemical reactions, specifically the “shrinking sphere” ( $1 - (1 - \alpha)^{1/3} = k \cdot t$ ), Yander ( $(1 - (1 - \alpha)^{1/3})^2 = k \cdot t$ ), and Crank-Ginstling-Brownstein ( $1 - 2/3\alpha - (1 - \alpha)^{2/3} = k \cdot t$ ) models [16]. The results of the calculations for the initial interval (0–5 h) are presented in Tables 4, 5.

As evidenced by the data presented in Tables 4, 5, the mathematical processing of the equations of formal kinetics for the degree of titanium extraction into solution ( $\alpha$ ) reveals a clear dependence between the results for Solutions 1, 2. This dependence is most accurately described by the equation of “shrinking sphere”. The graphical processing of the linearization of the results by this equation enabled the determination of the values of approximation reliability (Fig. 2). The corrected coefficient of determination ( $R^2$ ) for the 1<sup>st</sup> and 2<sup>nd</sup> Solutions is 0.992, while the Pearson correlation coefficient (PCC) is 0.997. The kinetic constant of the reaction for the 1<sup>st</sup> solution is  $k_1 = (9.29 \pm 0.4) \cdot 10^{-6}$ , for the 2<sup>nd</sup> Solution  $k_1 = (1.23 \pm 0.05) \cdot 10^{-5}$ .

In the second interval ( $\tau = 5\text{--}25 \text{ h}$ ), the mathematical calculations of the values according to the equations

Table 4  
Calculations using the “shrinking sphere”, Yander, Crank-Ginstling-Brownstein equations for Solution 1 ( $C_M(\text{NH}_4)^+ = 0.4 \text{ mol/L}$ ,  $C_M(\text{F})^- = 0.8 \text{ mol/L}$ ) in first interval ( $\tau = 5 \text{ h}$ )

Process time, s	Degree of extraction, $\alpha$	$1 - (1 - \alpha)^{1/3}$	$(1 - (1 - \alpha)^{1/3})^2$	$1 - 2/3\alpha - (1 - \alpha)^{2/3}$
0	0	0.00	0.00	0.00
3600	$0.08 \pm 0.04$	$0.03 \pm 0.02$	$0.00 \pm 0.00$	$0.00 \pm 0.00$
7200	$0.17 \pm 0.04$	$0.06 \pm 0.02$	$0.00 \pm 0.00$	$0.00 \pm 0.01$
10800	$0.28 \pm 0.04$	$0.10 \pm 0.02$	$0.01 \pm 0.01$	$0.01 \pm 0.01$
14400	$0.36 \pm 0.04$	$0.14 \pm 0.02$	$0.02 \pm 0.01$	$0.02 \pm 0.01$
18000	$0.41 \pm 0.04$	$0.16 \pm 0.02$	$0.03 \pm 0.01$	$0.02 \pm 0.01$

Table 5  
Calculations using the “shrinking sphere”, Yander, Crank-Ginstling-Brownstein equations for Solution 2 ( $C_M(\text{NH}_4)^+ = 0.4 \text{ mol/L}$ ,  $C_M(\text{F})^- = 0.9 \text{ mol/L}$ ) in first interval ( $\tau = 5 \text{ h}$ )

Process time, s	Degree of extraction, $\alpha$	$1 - (1 - \alpha)^{1/3}$	$(1 - (1 - \alpha)^{1/3})^2$	$1 - 2/3\alpha - (1 - \alpha)^{2/3}$
0	0	0.00	0.00	0.00
3600	$0.12 \pm 0.04$	$0.04 \pm 0.02$	$0.00 \pm 0.01$	$0.00 \pm 0.01$
7200	$0.23 \pm 0.04$	$0.08 \pm 0.02$	$0.01 \pm 0.01$	$0.01 \pm 0.01$
10800	$0.36 \pm 0.04$	$0.14 \pm 0.02$	$0.02 \pm 0.01$	$0.02 \pm 0.01$
14400	$0.46 \pm 0.04$	$0.19 \pm 0.02$	$0.03 \pm 0.01$	$0.03 \pm 0.01$
18000	$0.51 \pm 0.04$	$0.21 \pm 0.02$	$0.04 \pm 0.01$	$0.04 \pm 0.01$

of the “shrinking sphere”, Yander, and Crank-Ginstling-Brownstein were conducted in a similar manner.

A comparable mathematical analysis of the data using the aforementioned equations of formal kinetics for the specified time interval ( $\tau = 5\text{--}25$  h) revealed that the relationship between the degree of transformation and reaction time can be most accurately represented

in the coordinates of the “shrinking sphere” and Yander equations (Figs. 3, 4). For the 1<sup>st</sup> Solution: in the coordinates of the “shrinking sphere” equation the corrected coefficient of determination ( $R^2$ ) is 0.627, Pearson correlation coefficient (PCC) is 0.849, kinetic constant of reaction  $k_1 = (7.77 \pm 2.8) \cdot 10^{-7}$ ; in the coordinates of the Yander equation  $R^2$  is 0.831; PCC is

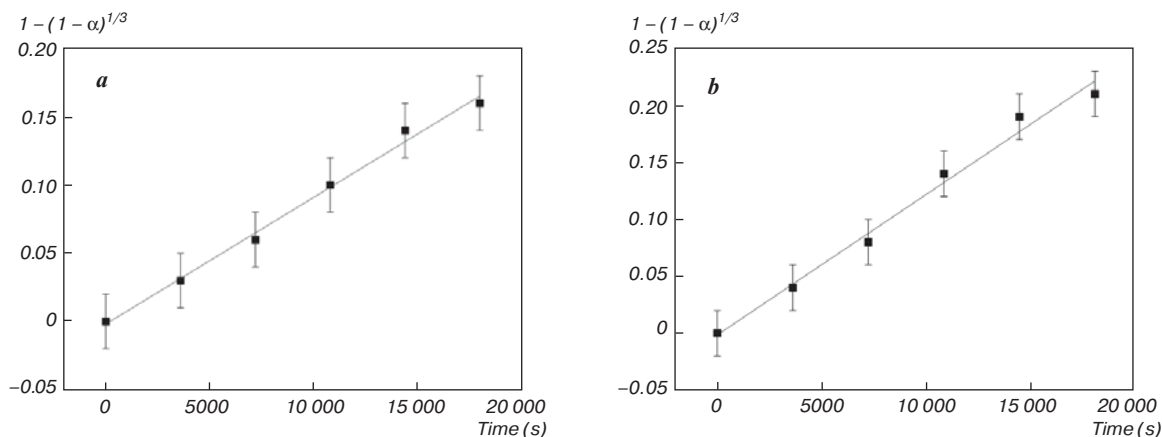


Fig. 2. Linearization of the graph in “shrinking sphere” coordinates in the first interval ( $\tau = 5$  h):  
 a –  $C_M(\text{NH}_4)^+ = 0.4$  mol/L,  $C_M(\text{F})^- = 0.8$  mol/L; b –  $C_M(\text{NH}_4)^+ = 0.4$  mol/L,  $C_M(\text{F})^- = 0.9$  mol/L

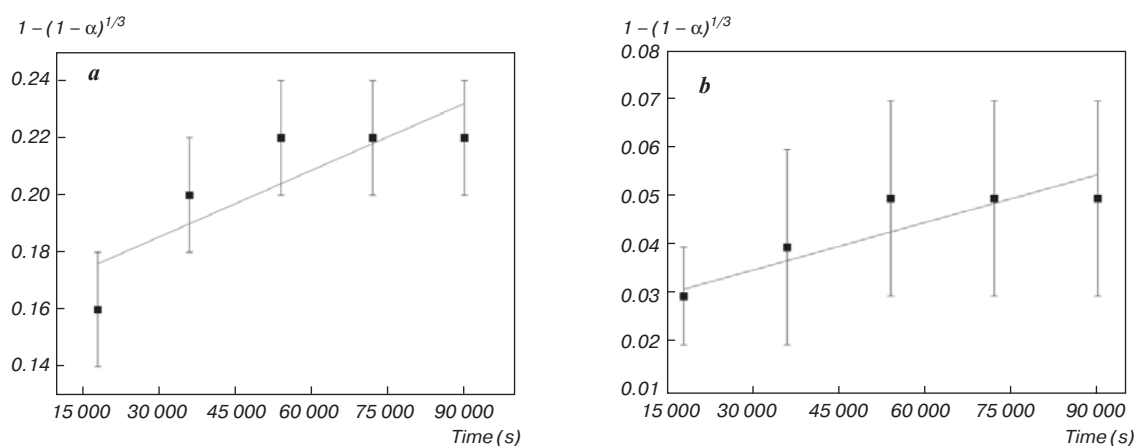


Fig. 3. Linearization of the graph for the 1<sup>st</sup> Solution ( $C_M(\text{NH}_4)^+ = 0.4$  mol/L,  $C_M(\text{F})^- = 0.8$  mol/L) in the second interval:  
 a – “shrinking sphere”; b – Yander equation

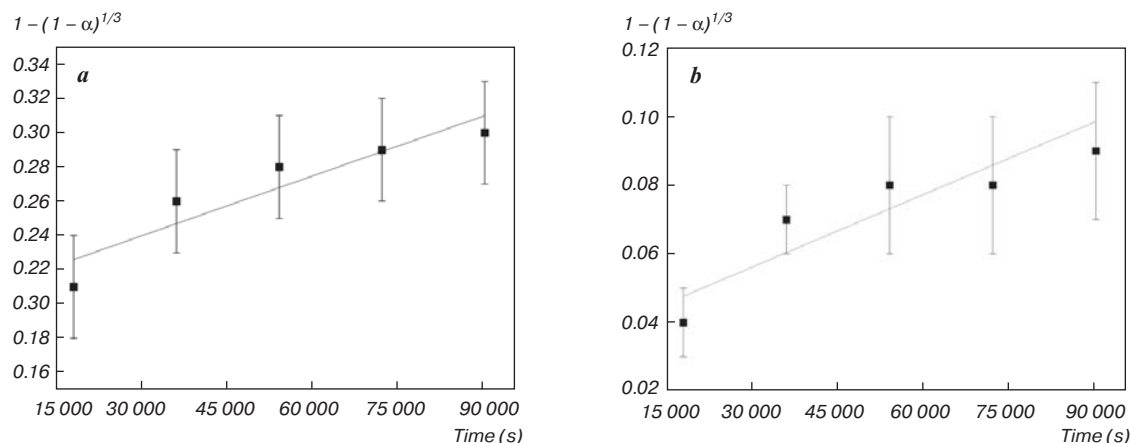


Fig. 4. Linearization of the graph for the 2<sup>nd</sup> Solution ( $C_M(\text{NH}_4)^+ = 0.4$  mol/L,  $C_M(\text{F})^- = 0.9$  mol/L) in the second interval:  
 a – “shrinking sphere”; b – Yander equation

Table 6

**Linearization analysis using the “shrinking sphere” and Yander equations for the 1<sup>st</sup> and 2<sup>nd</sup> Solutions in the second interval of 5-25 h.**

Type of Solution	Equation	R <sup>2</sup>	PCC	k1
1 <sup>st</sup> solution	“shrinking sphere”	0.627	0.849	$(7.77 \pm 2.8) \cdot 10^{-7}$
	Yander equation	0.831	0.935	$(3.25 \pm 0.7) \cdot 10^{-7}$
2 <sup>nd</sup> solution	“shrinking sphere”	0.838	0.937	$(1.20 \pm 0.3) \cdot 10^{-6}$
	Yander equation	0.720	0.889	$(7.07 \pm 2.1) \cdot 10^{-7}$

Table 7

**Value of apparent activation energy**

Type of solution	First interval	Second interval
1 <sup>st</sup> Solution	$E_a \in (30; 63)$ kJ/mol	$E_a \in (39; 71)$ kJ/mol
2 <sup>nd</sup> Solution	$E_a \in (30; 63)$ kJ/mol	$E_a \in (37; 70)$ kJ/mol

0.935, kinetic constant of reaction  $k_1 = (3.25 \pm 0.7) \times 10^{-7}$  (Table 6).

For the 2<sup>nd</sup> Solution, in coordinates of the contracting sphere equation, R<sup>2</sup> is 0.838; PCC is 0.937, and the kinetic constant of the reaction is  $k_1 = (1.20 \pm 0.3) \cdot 10^{-6}$ ; in coordinates of the Yander equation, R<sup>2</sup> is 0.720; PCC is 0.889, and the kinetic constant of the reaction is  $k_1 = (7.07 \pm 2.1) \cdot 10^{-7}$ .

The “shrinking sphere” equation (Gray-Weddington) can be applied in combustion or dissolution processes, whereby a particle of a reacting substance, undergoing a loss of mass, undergoes a reduction in size. Typically, the shrinking sphere equation is an effective means of describing the processes occurring within the kinetic region of a reaction. The Yander equation, in turn, describes the model of product layer growth on the particle. The accuracy of the experimental points on the graph of the Yander equation is contingent upon the thickness of the layer formed on the particle of the solid reaction product being significantly less than the radius of the unreacted nucleus. In consideration of the R<sup>2</sup> values presented in Table 6, it can be posited that the leaching process associated with Solution 1 is more accurately represented by the Yander equation. This suggests that the phenomenon in question is constrained by diffusion through the formed product layer. In the case of Solution 2, the process is better described by the contracting sphere equation, indicating that the kinetic step represents the limiting factor. It seems reasonable to posit that the addition of fluoride ions facilitates the dissolution of the products in question.

The apparent activation energy is expressed from the Arrhenius equation:

$$E_a = (\ln k_0 - \ln k_T) \cdot RT, \quad (3)$$

where:  $E_a$  – activation energy;  $k_0$  – pre-exponential multiplier;  $k_T$  – reaction rate constant;  $R$  – universal gas constant;  $T$  – temperature.

As evidenced by the experimental data presented by Melvin and Hughes [17], the majority of reactions occur at typical rates. The value  $\ln k_0 = 14.3$  corresponds to these

rates. In light of the aforementioned evidence, it can be reasonably assumed that  $\ln k_0$  falls within the range of 1 to 14.3. The temperature of the process is 295 K. Calculated by equation (3) values of activation energy  $E_a$ , corresponding to the leaching process in the interval  $\tau = 5$  h and  $\tau = 5-25$  h, are presented in Table 7.

In light of the activation energy, it can be posited that the response region is situated within the kinetic region. The linearization of experimental data using the equations of Gray-Waddington (“shrinking sphere”), Yander, and Histling-Braunstein demonstrated that the rate of the leaching process is constrained by two factors: the duration and concentration of the initial solution. These factors influence the leaching process by affecting the chemical reaction between the fluoride-containing solution and the titanium compounds present in the ore, as well as the diffusion of reagents through the film of reaction products and undissolved impurities. The leaching process can be impeded by the presence of insoluble products, such as  $(\text{NH}_4)_3[\text{FeF}_6]$  hexafluoroferrate (III) ammonium, which accumulate in layers as the reaction progresses.

## Conclusion

The kinetics of titanium leaching in fluorine-containing solutions has been the subject of study. It was determined that the extent of titanium extraction into the solution increases with time, reaching a maximum during leaching for 10 hours. The graph was linearized in “shrinking sphere” coordinates. In the initial five-hour period following leaching, the graph is linearized in accordance with the coordinates of the “shrinking sphere.” The results of the calculations for the second plot, spanning the range of 5 to 25 hours, are linearized in the coordinates of the Yander equation for Solution 1. In the case of Solution 2, the process is more accurately represented by the contracting sphere equation, which indicates the presence of a limiting kinetic stage. The limiting stage is dependent upon the duration of leaching and the composition of the leaching solution. The introduction of fluoride ions into the solution results in a shift towards the kinetic region of the reaction.

## Acknowledgment

*This study was supported by the Tomsk State University Development Programme (Priority-2030).*

## References

1. Chernysheva, L. V., Smelyanskaya G. A., Zaitseva G. M. Typomorphism of Magnetite and Its Use in the Search and Evaluation of Ore Deposits. Moscow: Nedra, 1981. 235 p.
2. Fominikh V. G. Urals Titanomagnetite Formations. *Urals Ore-Bearing and Ore Formations: Collection of Scientific Works*. Sverdlovsk: UrO AN SSSR, 1988. pp. 139–148.



3. Borisenko L. F., Delitsyn L. M. Prospects for the Development of Titanium Raw Materials in Russia. *Russian Mining Industry*. 1996. Iss. 4. pp. 23–25.
4. Kalinnikov V. T., Nikolaev A. I., Kotsar M. L. Non-Traditional Rare-Metal Raw Materials of the Kola Peninsula: Substantiation and Prospects of Their Use in Technology. *Mining Informational and Analytical Bulletin*. 2007. S1. pp. 13–23.
5. Lattard D., Engelmann R., Kontny A., Sauerzapf U. Curie Temperatures of Synthetic Titanomagnetites in the Fe – Ti – O System: Effects of Composition, Crystal Chemistry, and Thermomagnetic Methods. *Journal of Geophysical Research: Solid Earth*. 2006. Vol. 111, B12S28.
6. Moskowicz B. M., Jackson M., Chandler V. Geophysical Properties of the Near-Surface Earth: Magnetic Properties. In: *Treatise on Geophysics, 2<sup>ed</sup>*. Elsevier, 2015. pp. 139–174.
7. Reznichenko V. A., Shabalin L. I. Titanomagnetites: Deposits, Metallurgy, Chemical Technology. Moscow: Nauka, 1986. 291 p.
8. Xu C., Zhang Y., Liu T. Huang J. Characterization and Pre-Concentration of Low-Grade Vanadium-Titanium Magnetite Ore. *Minerals*. 2017. Vol. 7, Iss. 8. 137.
9. Smirnov L. A., Deryabin Yu. A., Shavrin S. V. Metallurgical Processing of Vanadium-Containing Titanomagnetites. Chelyabinsk: Metallurgy, Chelyabinskoye Otdeleniye, 1990. 254 p.
10. Taylor P. R., Shuey S. A., Vidal E. E., Gomez J. C. Extractive Metallurgy of Vanadium-Containing Titaniferous Magnetite Ores: a Review. *Mining, Metallurgy & Exploration*. 2006. Vol. 23. pp. 80–86.
11. Li X., Pu J. The Latest Developments of Integrated Utilization on Panzhihua High Titanium-Bearing BF Slag. *Iron Steel Vanadium Titan*. 2011. Vol. 32, Iss. 2. pp. 10–14.
12. Dmitriev A. N., Smorokov A. A., Kantaev A. S., Nikitin D. S., Vit'kina G. Yu. Fluorammonium Method of Titanium Slag Processing. *Izvestiya. Ferrous Metallurgy*. 2021. Vol. 64, Iss. 3. pp. 178–183.
13. Andreev A. A. Fluoride Technology for the Production of Pigment Titanium Dioxide. *Fluoride technologies: Proceedings report of All-Russian Scientific and Practical Conference. Tomsk, 25–26 June 2009*. p. 27.
14. Gordiyenko P. S., Sheka S. A., Bakeyeva N. G., Pashnina E. V., Usoltseva T. I., Kolzunov V. A. Hydrofluoride Method of Processing Ilmenite Concentrates. *Mining Information and Analytical Bulletin*. 2010. Iss. S4. pp. 278–288.
15. Sachkov V., Nefedov R., Orlov V., Medvedev R., Sachkova A. Hydrometallurgical Processing Technology of Titanomagnetite Ores. *Minerals*. 2018. Vol. 8, Iss. 1. 2.
16. Dyachenko A. N., Shagalov V. V. Chemical Kinetics of Heterogeneous Processes: a Training Manual. Tomsk: Tomsk Polytechnic University Publishing House. 2014. 102 p.
17. Cherepanov V. A. Chemical Kinetics. Ekaterinburg: Izdatelstvo Uralskogo Universiteta, 2016. 128 p.